

Supporting Information

Molybdenum Disulfide Catalytic Coatings via Atomic Layer Deposition for Solar Hydrogen Production from Copper Gallium Diselenide Photocathodes

Thomas R. Hellstern, David W. Palm, James Carter, Alex D. DeAngelis, Kimberly Horsley, Lothar Weinhardt, Wanli Yang, Monika Blum, Nicolas Gaillard, Clemens Heske, Thomas F. Jaramillo*

Dr. T.R. Hellstern, D.W. Palm, Prof. T.F. Jaramillo
Department of Chemical Engineering, Stanford University
443 Via Ortega, Stanford, California 94305, United States

J. Carter, Dr. L. Weinhardt, Dr. M. Blum, Prof. C. Heske
Department of Chemistry and Biochemistry, University of Nevada Las Vegas (UNLV)
4505 Maryland Pkwy, Las Vegas, Nevada, 89154-003, United States

A.D. DeAngelis, Dr. K. Horsley, Dr. N. Gaillard
Hawaii Natural Energy Institute (HNEI), University of Hawaii at Manoa
1680 East-West Rd, POST 109, Honolulu, Hawaii 96822, United States

Dr. L. Weinhardt, Prof. C. Heske
Institute for Photon Science and Synchrotron Radiation (IPS), Karlsruhe Institute of Technology (KIT)
Hermann-v.-Helmholtz-Platz 1, 76344 Eggenstein-Leopoldshafen, Germany

Institute for Chemical Technology and Polymer Chemistry (ITCP), Karlsruhe Institute of Technology (KIT)
Engesserstr. 18/20, 76128 Karlsruhe, Germany

Dr. W. Yang, Dr. M. Blum
Advanced Light Source (ALS), Lawrence Berkeley National Laboratory
1 Cyclotron Road, Berkeley, California 94720, United States

Prof. T.F. Jaramillo*
SUNCAT Center for Interface Science and Catalysis, SLAC National Accelerator Laboratory
2575 Sand Hill Road, Menlo Park, California, 94025, United States

Corresponding Author

Thomas F. Jaramillo
Department of Chemical Engineering, Stanford University
443 Via Ortega, Stanford, California 94305, United States
*jaramillo@stanford.edu

Contents

1. Lamp Calibration to AM1.5G
2. Figure S1: Linear growth curve for MoO_x ALD
3. Figure S2: Onset Potential Determination
4. Figure S3: X-ray diffraction spectra of CGSe/FTO
5. Figure S4: Transmittance data for CGSe and MoS₂/TiO₂/CdS/CGSe on FTO
6. Figure S5: Optimization of sulfidization time
7. Figure S6: HER catalytic data for MoS₂/TiO₂/FTO electrodes
8. Hydrogen production calculation
9. Figure S7: Absorptance data for CGSe electrodes and CdS and MoS₂/TiO₂/CdS on quartz
10. Figure S8: Dark LSVs for MoS₂/TiO₂/CdS/CGSe electrode during durability study

Lamp Calibration to AM1.5G

Using an Ocean Optics Jaz EL 200-XR1 spectrometer, the absolute irradiance output from the Xe lamp was measured as illuminated through the quartz window of the cell, without solution. The irradiance incident at the detector surface was manipulated by controlling the working distance between the lamp and the detector surface. This irradiance was considered to be calibrated to AM1.5G when the density of above-bandgap photons (those with photon energy exceeding the bandgap energy of the material) was equal to the density of above-bandgap photons in the AM1.5G solar spectrum, calculated using NREL's SMARTS2 worksheet.¹⁻³ The photon density (as a fraction of the AM1.5G solar output) is estimated to vary by up to 5% from sample to sample due to the imprecision of manually aligning the electrode at the same distance from the lamp as the detector.

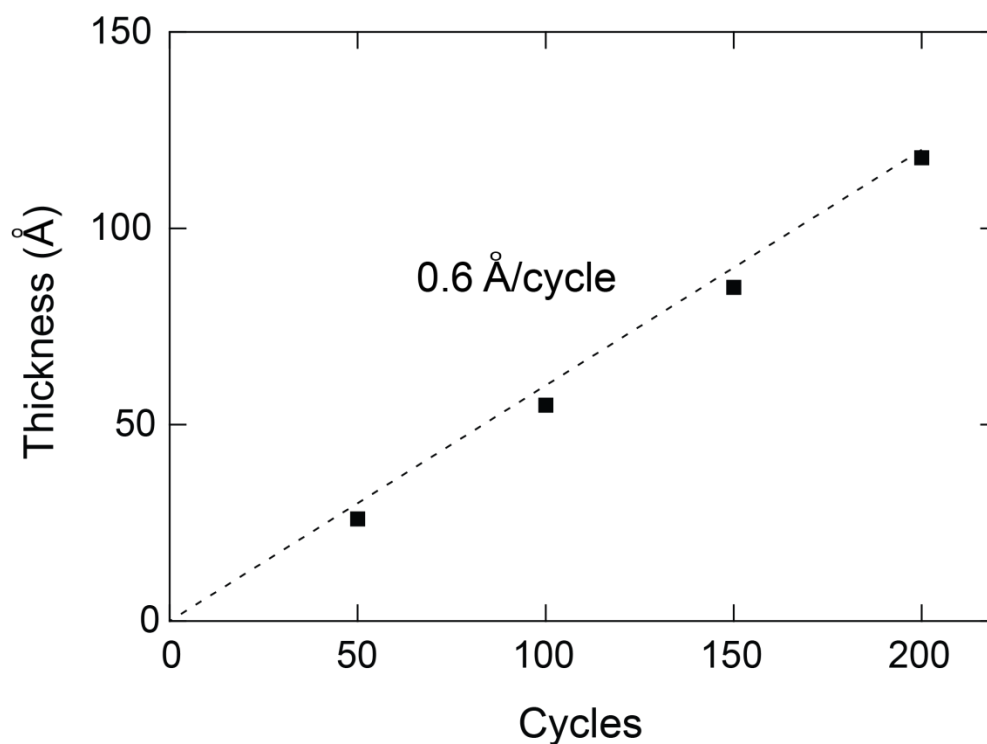


Figure S1: Linear growth curve for MoO_x ALD, showing a growth rate of nearly 0.6 Å per cycle at 165°C (line intended as a guide for the eye). The thickness was determined by spectroscopic ellipsometry, and Mo(CO)₆ and O₂ plasma were used as ALD precursors. The Mo precursor was pre-heated to 70°C. Each cycle consisted of a 2 s pulse of Mo precursor prior to a 10 s purge in Ar carrier gas (260 sccm) followed by an O₂ plasma phase involving O₂ flowed at 20 sccm with the RF plasma generator set to 300 W for 20 s, followed by a 5 s purge time.

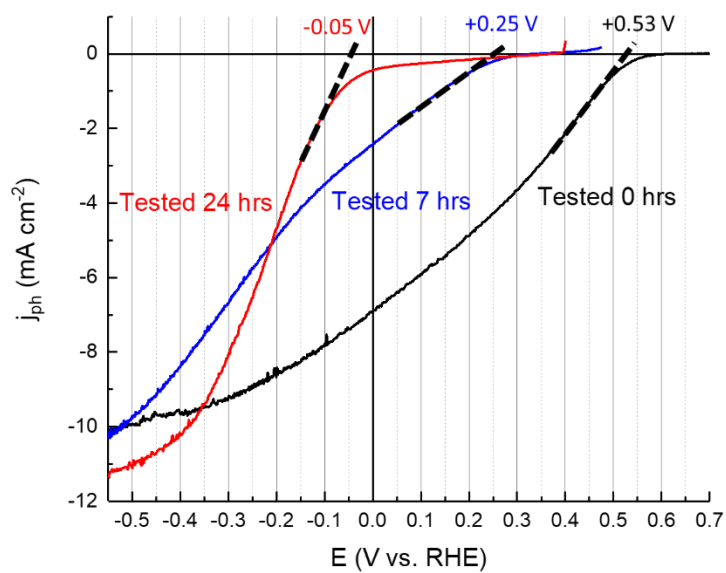


Figure S2: Determination of the onset potential for three LSV experiments performed on MoS₂/TiO₂/CdS/CGSe electrodes. The data are reproduced from Figure 3a.

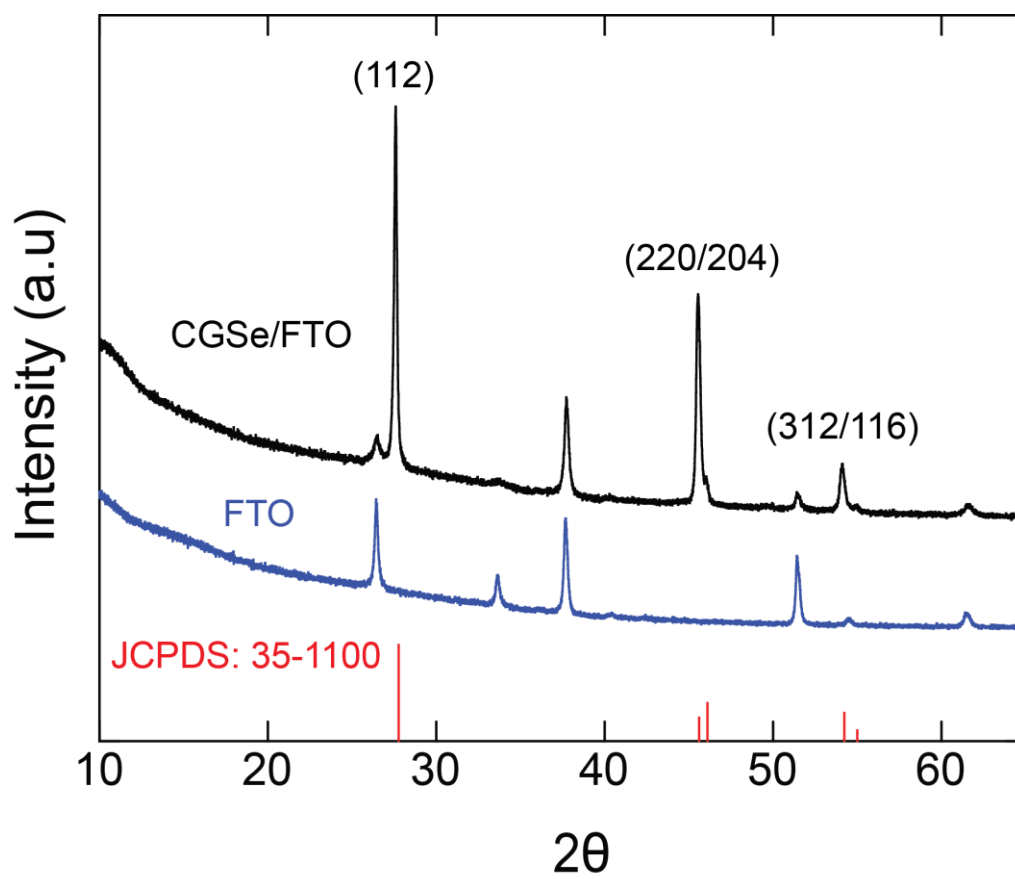


Figure S3: X-ray diffractograms of CGSe/FTO (black) and FTO (blue). Reference spectrum 35-1100 for CuGaSe₂ is also provided.⁴

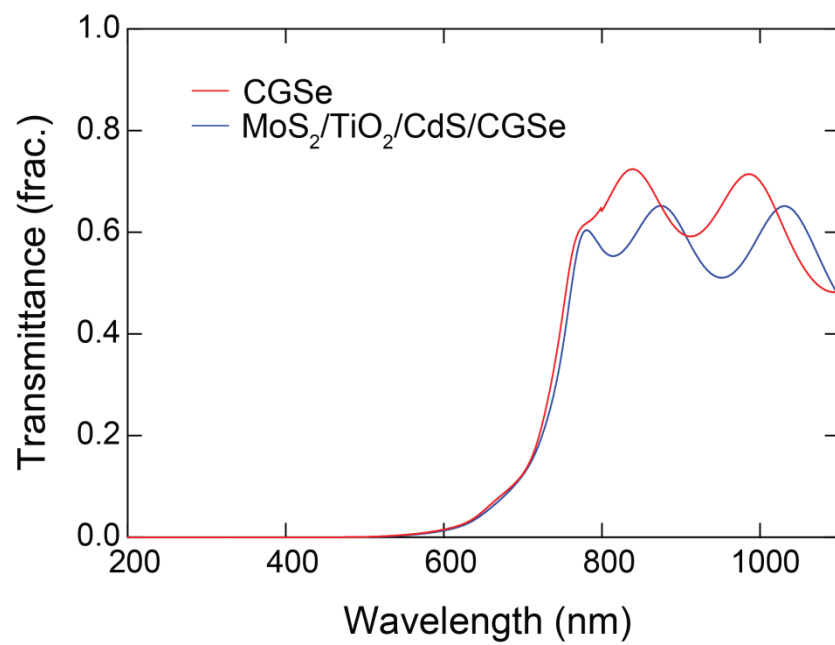


Figure S4: Transmittance data for CGSe (red) and MoS₂/TiO₂/CdS/CGSe on FTO (blue).

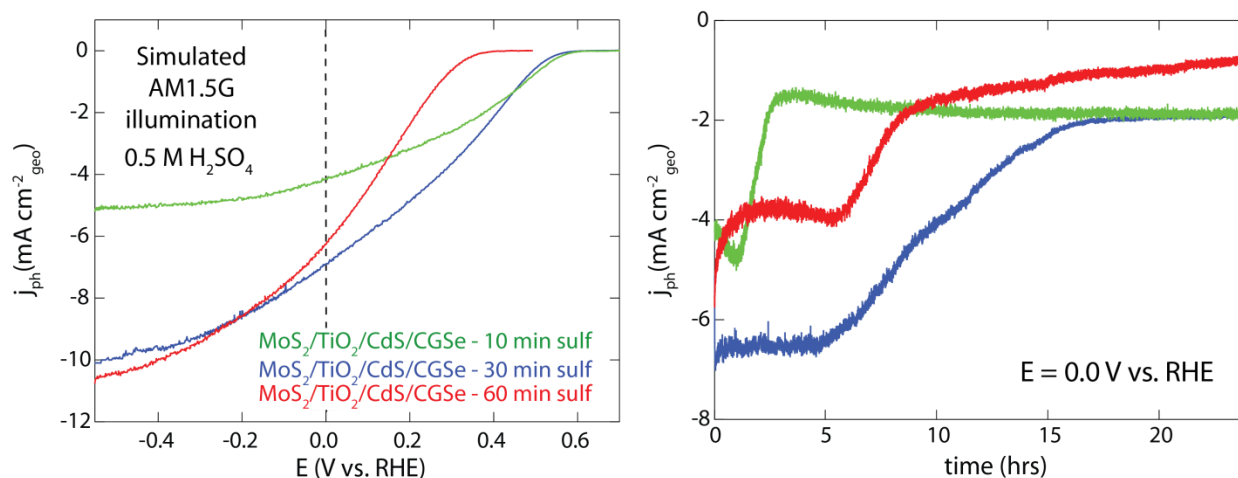


Figure S5: Optimization of sulfidization time. $\text{MoS}_2/\text{TiO}_2/\text{CdS}/\text{CGSe}$ electrodes were formed by varying thermal sulfidization time: 10 min (green), 30 min (blue), and 60 min (red). LSVs before stability testing (left) and 24 hr stability tests at 0.0 V vs. RHE (right) were performed to assess optimal sulfidization conditions.

A sulfidization time of 30 minutes was determined to optimize both activity and durability of the $\text{MoS}_2/\text{TiO}_2/\text{CdS}/\text{CGSe}$ photocathode. The initial LSV for the 30 minute sulfidized electrode results in the best combination of early onset and high photocurrent density. Short sulfidization times lead to low saturation photocurrent density. Longer sulfidization times lead to higher current densities, but also result in loss of photovoltage and fill factor (perhaps due to worsening catalytic activity, as shown in Figure S5). The loss of photovoltage could be due to loss of CdS/CGSe junction fidelity caused by Cu/Cd interdiffusion at 200°C. The 30-minute sulfidization also provides the best stability to electrodes, as it is important to balance (1) complete formation of a conformal MoS_2 coating and (2) high photovoltage that results in high current density at 0.0 V vs. RHE.

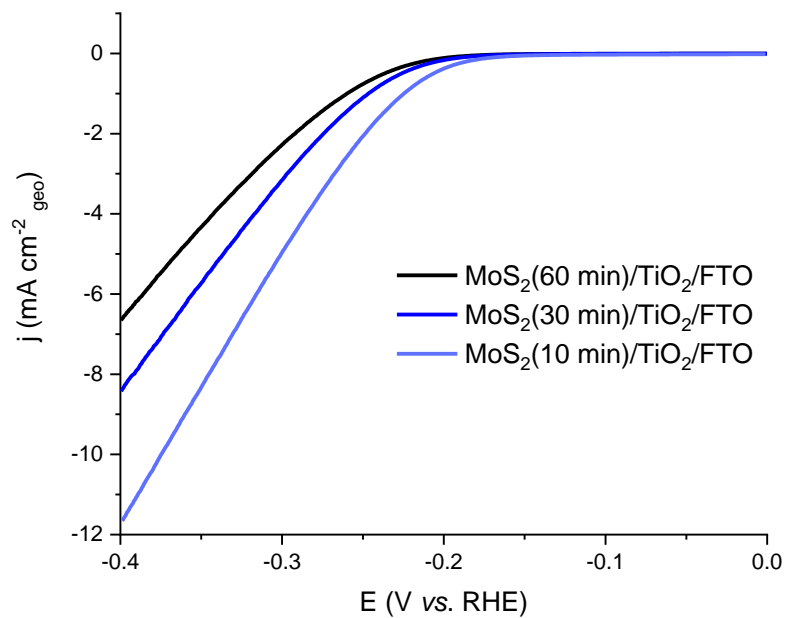


Figure S6: Effect of sulfidization time on HER catalytic performance of MoS₂/TiO₂/FTO electrodes: 10 min (light blue), 30 min (deep blue), and 60 min (black). The LSVs were performed in 0.5 M H₂SO₄ with a Hg/HgSO₄ reference electrode, Ir/IrO_x counter electrode, and with H₂ continuously bubbling through the solution.

Hydrogen production calculation

Hydrogen production is the dominant contributor to the photocurrent generated over the course of the experiment. This is evidenced by the sustained bubble formation at the electrode surface and the substantial total charge passed, 10^{-3} mol e^- (average of 4 mA cm^{-2} , 0.3 cm^2 area, 24 hrs x 3600 s per hour) over the course of durability testing. This amount of charge is four orders of magnitude greater than that which might otherwise have come from photoelectrode corrosion. The photoelectrode predominantly consists of CGSe (density of 5 g/cm^3 , 0.3 cm^2 area, thickness of 1 μm , molecular weight of 291 g/mol), equivalent to approximately 10^{-7} mol CuGaSe_2 .

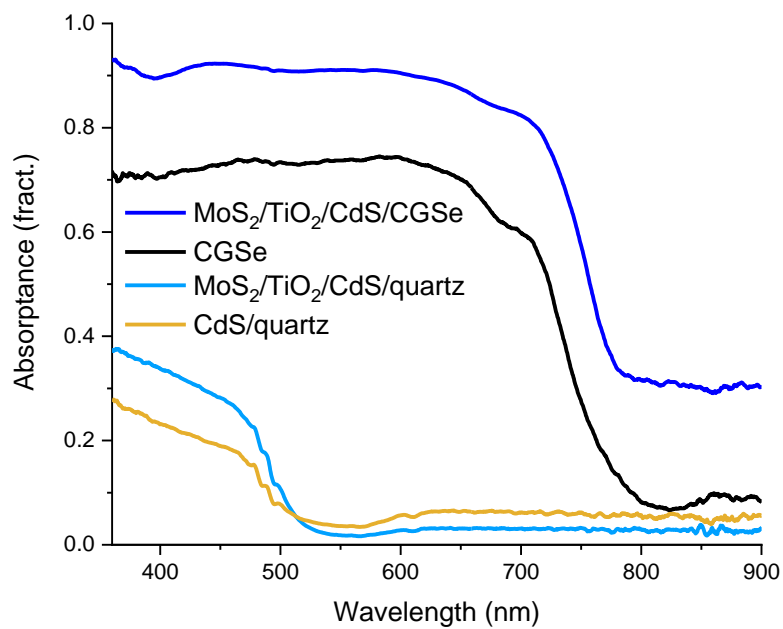


Figure S7: Absorbance data for CGSe electrodes and CdS and MoS₂/TiO₂/CdS on quartz.

The MoS₂/TiO₂/CdS catalytic/interface/buffer layer absorbs roughly 20% of the photons above 500 nm.

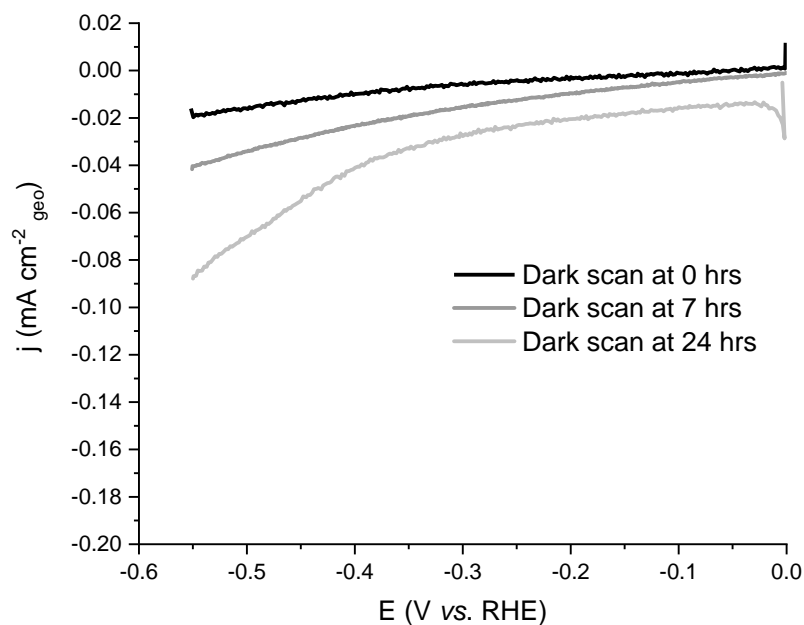


Figure S8: LSVs taken in the dark for the MoS₂/TiO₂/CdS/CGSe samples investigated in Figure 3. While the currents are small in comparison to the observed photocurrents, there appears to be a reductive wave (onset near -0.4 V *vs.* RHE) that increases with the duration of durability testing. This feature becomes very noticeable after 24 hrs of continuous testing and may be indicative of Cd²⁺ reduction, with the standard electrode potential of this reaction being -0.40 V *vs.* NHE.⁵

References

1. Gueymard, C. SMARTS: Simple Model of the Atmospheric Radiative Transfer of Sunshine. National Renewable Energy Laboratory. <https://www.nrel.gov/rredc/smarts/>. Accessed 12 November 2018.
2. Gueymard, C. Parameterized Transmittance Model for Direct Beam and Circumsolar Spectral Irradiance. *Solar Energy* **2001**, *71*, 325–346.
3. Gueymard, C. SMARTS2, A Simple Model of the Atmospheric Radiative Transfer of Sunshine: Algorithms and Performance Assessment. Florida Solar Energy Center. Cocoa, FL, 1995.
4. *CuGaSe2*, JCPDS card No. 35-1100; JCPDS International Centre for Diffraction Data: Swarthmore, Pennsylvania, USA.
5. Bard, A. J.; Faulkner, L. R. *Electrochemical Methods: Fundamentals and Applications*, 2nd edition; Wiley: New York, 2001.